Photodissociation Quantum Yield of Iodine in the Low-, Medium-, and High-Density Fluids Studied by the Transient Grating Method

H. Ooe, Y. Kimura,* M. Terazima, and N. Hirota

Department of Chemistry, Graduate School of Science, Kyoto University, Kyoto 606-8502, Japan

Received: April 26, 1999; In Final Form: July 20, 1999

The transient grating (TG) method has been applied to the determination of the photodissociation quantum yield (ϕ_d) of iodine in various fluids at low-, medium-, and high densities. After a nanosecond laser excitation at 532 nm, the thermal grating created by fast processes such as excess energy relaxation, primary geminate recombination, and secondary geminate recombination appears as a fast rise of the TG signal, and the thermal grating created by the nongeminate recombination process appears as a slow rise of the TG signal. By comparison of the relative intensities of these signals, ϕ_d has been determined. We have demonstrated that the species grating and the volume grating are negligible in the TG signal in fluids such as argon at 323 K, krypton at 293 K, and liquid solvents at room temperature. Our results of ϕ_d in these solvents show density dependence similar to those previously measured by the transient absorption method (Dutoit, J.-C.; et al. *J. Chem. Phys*. **1983**, *78*, 1825. Luther, K.; et al. *J. Phys. Chem*. **1980**, *84*, 3072.), although our results are larger quantitatively. The diffusion model (Otto, B.; et al. *J. Chem. Phys*. **1984**, *81*, 202) works well for interpretation of the density dependence, although modifications of the theory are required to get a quantitative agreement. In xenon, sulfur hexafluoride, carbon dioxide, ethane, and nitrous oxide, which have critical temperatures near the temperature of this experiment (323 or 333 K), we observed a density dependence of ϕ_d similar to that in argon, while a significant decrease of ϕ_d in the low-density region of carbon dioxide, ethane, and nitrous oxide was reported previously (Zellweger, J. M.; et al. *J. Chem. Phys*. **1980**, *72*, 5405. Otto, B.; et al. *J. Chem. Phys*. **1984**, *81*, 202.). Discussion on the origin of the difference is presented on the basis of the intermolecular potential estimated by the solubility data.

1. Introduction

The photodissociation and recombination reaction is one of the simplest reactions that reflects various interesting aspects of solvent effects such as excess energy relaxation at higher electronic states, geminate recombination due to solvent friction, vibrational energy relaxation in recombination processes, and so on. The solvent effect that prevents dissociation is often termed the "cage effect". The photodissociation quantum yield ϕ_d, which is defined as the fraction of nongeminate recombination, is a representative value of the solvent cage effect. It is easy to imagine that ϕ_d becomes small with a strengthening of the solvent cage effect.

A simple diatomic molecule such as iodine is a primary model system for the study of the photodissociation reaction in solution, and numerous studies have been performed since the work of Ravinowitch and Franck.[1] The first systematic study on the photodissociation quantum yield was performed by Noyes et al.[2−4] They measured the solvent viscosity dependence and the excitation wavelength dependence of ϕ_d of iodine by the radical trapping method. They discussed the results on the basis of a simple model that the atoms produced by the photodissociation start to separate in exactly opposite directions with a total kinetic energy in excess of the normal thermal energy. However, it is now realized that the process is not as simple as predicted by such a model partly because several electronic states are coupled with each other.

The photodissociation and recombination processes of iodine excited in the visible region are briefly summarized by the following four steps (see Figure 1a).

(1) By use of visible light, iodine is excited to the bound B state, the dissociative Π_u state, or the A/A′ state depending on the wavelength for excitation.[5] For example, when excited at 532 nm (the wavelength that we use mainly in this work), the population of these states are reported to be 87% in the B state and 13% in the Π_u state. The wave-packed dynamics in the B state and the following electronic predissociation after the photoexcitation have been recently investigated intensively in clusters,[6−8] gases,[9−11] supercritical fluids,[12−17] liquids,[18,19] and solids.[20] Although the rate of the electronic predissociation is dependent on the environment, it is generally within the picosecond time scale.

(2) After the transition to the dissociative state, a fraction of the separating atoms recombine geminately on the A/A′ potential surface or on the ground-state X due to the collisional interaction with solvent molecules, and vibrationally highly excited molecules are produced. This process is called primary geminate recombination in a sense that the iodine molecule does not break out of the solvent cage. The appearance of the highly excited molecules is reported to occur within 2 ps or less in liquid solution.[21] The vibrationally hot molecules are cooled because of the interaction with the solvent molecule. The vibrational relaxation rate is strongly dependent on the solvent and the electronic state of iodine. In the ground-state X, the time constant

10.1021/jp991337u CCC: $18.00
Published on Web 09/03/1999

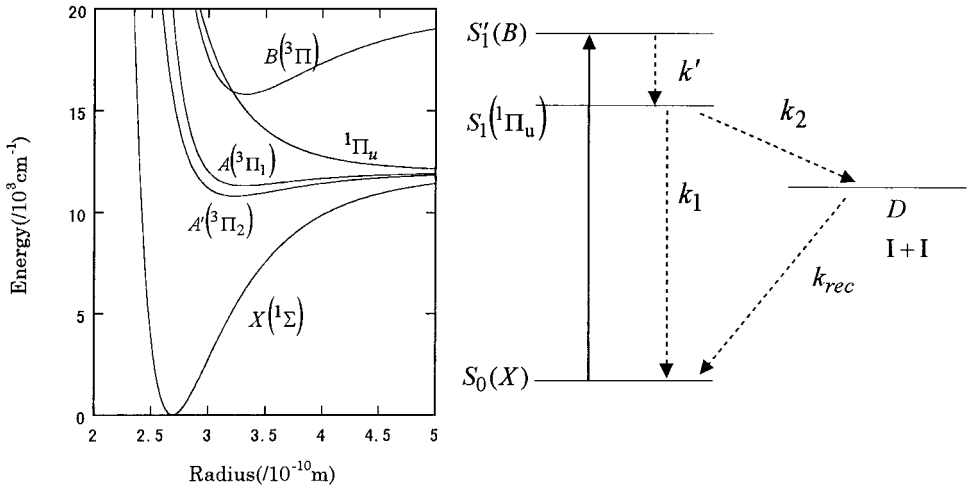

Figure 1. (a) Schematic drawing for simplified electronic energy surfaces of iodine. (b) Four-state kinetic model for the dissociation and the recombination reaction.

of the decay is typically 50−200 ps in liquid solvents.[22] The vibrational relaxation rate in the A/A′ state is much faster than in the ground-state under the similar experimental conditions.[17] The molecule in the A/A′ state escapes to the ground-state potential surface via a solvent-induced nonadiabatic transition with a time scale of 100 ps to nanoseconds.[23−25]

(3) Another fraction of the separating atoms succeed in breaking out of the solvent cage, and they diffuse out of at least one solvent molecule. These atoms may geminately diffuse back and recombine with the other atom of the same parent molecules. This process is called the secondary geminate recombination. This time scale is reported to be 200 ps in Ar at 200 bar and 323 K.[16] After the recombination, a vibrationally excited molecule is created, from which follows the vibrational energy relaxation as mentioned above.

(4) The remaining fraction of the atoms escape from the solvent cage and diffuse in the solvent. They are able to recombine with other separated atoms only when they happen to meet another atom. This process is called nongeminate recombination. This process is mainly diffusion-controlled and much slower than the primary and the secondary geminate recombination processes, and the time scale is larger than microseconds.

The photodissociation quantum yield ϕ_d does not contain detailed information on the earlier dynamics of iodine after the photoexcitation. However, it is still instructive to study ϕ_d under various experimental conditions, especially over a wide solvent density region from gaslike density to liquidlike density. The process described above is strongly influenced by collision with solvent molecules and the diffusivity of the iodine molecule. When the solvent density is changed by using supercritical fluids, it is possible to examine these processes clearly.

Extensive studies of ϕ_d in fluids over wide solvent densities and species were performed by the groups of Troe and van den Bergh nearly 20 years ago.[26−36] They have measured the recombination rate and ϕ_d in a variety of solvent fluids by transient absorption experiments using nanosecond or subnanosecond lasers and discussed their results on the basis of a simple diffusion-controlled mechanism. Their treatment is simple in comparison with various theoretical treatments such as stochastic dynamics or molecular dynamics simulation[37−42] but still instructive in grasping the overview that governs the mechanism of the dissociation and recombination dynamics. In their model, the recombination rate k_{rec} and the photodissociation quantum yield ϕ_d are given by the following equations:[30]

$$k_{rec} = 4\pi RDN_A \frac{k_{rec}^g}{k_{rec}^g + 4\pi RDN_A} \quad (1)$$

$$\phi_d = \frac{4\pi RDN_A}{k_{rec}^g + 4\pi RDN_A} \quad (2)$$

where D is the diffusion coefficient of iodine atom, R the collision distance where the iodine atoms make an encounter complex, and N_A Avogadro's number. k_{rec}^g is the recombination rate constant in the absence of diffusion control and considered to be limited by the energy relaxation rate in the ground state.

Troe et al. considered two limiting cases: a lower-density region and a higher-density region. In the case of the lower-density region where $k_{rec}^g \ll 4\pi RDN_A$, k_{rec} is approximately equal to k_{rec}^g. In such a density region, k_{rec} is linearly dependent on the solvent density (ρ).[26] Therefore, k_{rec}^g is given as

$$k_{rec}^g \propto \rho \propto D^{-1} \quad (3)$$

since the diffusion coefficient is inversely dependent on the solvent density in the low-density gases. In the case of the higher-density region where $k_{rec}^g \gg 4\pi RDN_A$, the quantum yield is correlated with D as

$$\phi_d \propto D^2 \propto \eta^{-2} \quad (4)$$

This is explained by eq 2 assuming $k_{rec}^g \propto D^{-1}$. This type of diffusion model explains well their results on the recombination rate constant over a wide solvent density region and ϕ_d in solvents such as krypton (Kr) and Xe. On the other hand, in fluids such as carbon dioxide (CO_2), ethane (C_2H_6), and nitrous oxide (N_2O), the values of ϕ_d were much lower than those predicted by the difffusion model (eq 4), even in a very low solvent density region. Troe et al. have concluded that this large

cage effect might come from formation of a complex I_2M,[30] where M denotes the solvent molecule. They assumed that this type of complex can lose the excess energy in I_2 by desorption of the solvent molecule (i.e., $I_2M \rightarrow I_2 + M$) with a probability γ^{cl}. By determining the complex concentration with an appropriate intermolecular potential, they could reproduce their experimental results at 581 nm excitation using $\gamma^{cl} = 0.7$.

However, the large value of γ^{cl} has not been explained well until now. To ensure their assumption, they referred to the cases of the van der Waals complex, where the one-atom cage effect has been observed.[43−48] For example, after the excitation of the B state dissociation level of the I_2-Ar cluster, the emission from the B state is observed,[48] which is interpreted as vibrational predissociation of the van der Waals cluster. This kind of vibrational predissociation has also been theoretically investigated by several authors.[49−51] However, the situation is somewhat different in the case of fluids around room temperature. After the iodine and solvent complex excited to the B state vibrationally predissociates, the iodine molecule still has a large energy in the B state relative to the ground state. In an environment where successive collisions with solvent molecules are possible, the electronic predissociation is induced by collision with solvent molecules.[15] Therefore, another mechanism is required to explain the decrease of ϕ_d. Although Dardi and Dahlr suggest a possible existence of a 1:1 complex in ethane around room temperature, they could not prove the factor of γ^{cl}.[52] We believe that ϕ_d of iodine is still an open problem and that it is worthwhile to reinvestigate the value by different experimental methods.

Recently, transient grating (TG) spectroscopy[53] has been applied to the measurement of ϕ_d with a nanosecond time resolution. This method detects the thermal energy dissipated by the photochemical processes. Zhu and Harris have demonstrated that this method is useful in determining ϕ_d, the recombination rate constant, and the enthalpy of the recombination reaction.[54,55] There are two kinds of rises in the TG signal for a system with photodissociation and recombination processes. The fast processes after photoexcitation such as the excess energy relaxation process, and the primary and the secondary geminate recombination processes are observed as a fast rise with a system response time when a nanosecond pulsed laser is used. Nongeminate recombination is observed as a slow rise over a microsecond time scale. Zhu and Harris determined ϕ_d for iodine from the saturation intensity estimated by the power dependence of the relative intensity of the slow-rise part.[54] In this procedure, however, a detailed knowledge of the excitation beam profile is required and the alignment must be kept rigorously the same during several measurements. It is quite difficult to apply this method directly to the measurement of ϕ_d in the high-pressure fluids over a wide solvent density region.

We have extended and simplified their analysis and already proved that our procedure is well applicable to a system in liquid solution.[56] This simplified analysis has an advantage that we can easily determine ϕ_d from the intensity ratio of the fast rise to the slow rise by measuring only one signal transient if we know the reaction enthalpy. Here, we applied this simplified method to determine ϕ_d of iodine in high-pressure fluids in order to study the cage effect. Our results in fluids such as CO_2, C_2H_6, and N_2O are quite different from those measured by the transient absorption method especially from the low-density region near the gaseous phase to the medium-density region near the critical density. In our results, little characteristic dependence on the solvent species is observed.

2. Theory

After the photoexcitation of iodine with a 532 nm laser, most earlier events except for the nongeminate recombination occur within a few nanoseconds in the liquid phase. In this case, the four-state diagram depicted by Zhu and Harris is applicable to the photodissociation and recombination dynamics of iodine (see Figure 1b). On the other hand, in fluids from the low-density to medium-density regions, the situation may be somewhat different. It has been proved that process 1 mentioned in the Introduction is much faster than a few tens of nanoseconds of our system response. The differences lie in the vibrational energy relaxation rate and the lifetime of the A/A′ state. Harris and co-workers have studied the vibrational energy relaxation rate in Xe from the medium-density to the high-density regions and found that the isolated binary collision model is applicable.[57] According to their study, the half period of the energy relaxation time at $\rho_r = 1.6$ in Xe is about 7 ns, where ρ_r is the reduced density by the critical density of the solvent. If we estimate the energy relaxation time at $\rho_r = 0.2$ (which is the lowest density we have measured) simply by the factor of the solvent density, a relaxation time of 56 ns is expected in Xe. We consider this to be sufficiently faster than the nongeminate recombination rate we have measured (ca. 1 microsecond). Although no other information is available, the energy relaxation rate in molecular solvents used in this study is expected to be much faster than the case of atomic solvents.[22]

The lifetime of the A/A′ state in lower density gases has not been well studied until now either. Harris and co-workers demonstrated that the lifetime of this state in Xe is around 9 ns at 280 K and could not detect meaningful density dependence from $\rho_r = 1.6$ to $\rho_r = 2.7$.[57] The study by Zewail et al. indicates that the lifetime of the A/A′ state in rare gas solvents is longer than 1 ns up to around $\rho_r = 2.2$.[16] Miller et al. reported that the lifetime of the A/A′ state in gaseous solvents is linearly dependent on the solvent density.[58] According to their results, the lifetime of the A/A′ state is about 20 ns in Ar at $\rho_r = 0.3$ if we can extrapolate their result up to this density. This lifetime is much shorter than the nongeminate recombination rate.

In the following, we assume that the reaction scheme is depicted by the four-state model as shown in Figure 1b. In this model, the rate constants k', k_1, and k_2 are assumed to be faster than the system response. We have simplified the treatment by Zhu and Harris, which was previously reported in detail.[56] Here, we briefly explain the outline of the theory and make some extensions including the factors that were neglected in the previous work.

In the TG measurement, the sample solution is irradiated by two laser beams crossing at the same time. This creates a light interference pattern in the sample solution, and iodine is excited according to the interference pattern. Successive photodissociation and recombination dynamics are monitored by the diffraction of a probe beam because of this grating. We assume that the intensity of the TG signal can be expressed as follows:[53]

$$I_{TG} \propto (\Delta n)^2 + (\Delta k)^2 \tag{5}$$

where Δn is the peak-null difference of the refractive index and Δk is the peak-null difference of the absorption coefficient, respectively. Δn is generally expressed as a sum of contributions from the thermal (Δn_{th}), population (Δn_{pop}), and

volume (Δn_V) gratings. Δk consists of only the population grating:

$$\Delta n = \Delta n_{th} + \Delta n_{pop} + \Delta n_V \quad (6)$$

$$\Delta k = \Delta k_{pop} \quad (7)$$

where Δn_{th} is caused by the thermal energy, Δn_{pop} by the change of the molecular refractive index, Δn_V by the reaction volume change ΔV, and Δk_{pop} by the change of the absorption coefficient, respectively.

Δn_{th} is explicitly expressed as

$$\Delta n_{th}(t) = \frac{dn}{dT}\frac{1}{\rho C_p}\left[Q_f \exp(-D_{th}q^2 t) + \frac{dQ_s(t)}{dt} * \exp(-D_{th}q^2 t)\right] \quad (8)$$

where the first term in the bracket corresponds to the fast heat and the second term to the slow heat. C_p, D_{th}, and q are the isobaric heat capacity, the thermal diffusivisty, and the grating lattice vector, respectively. The asterisk (*) denotes the convolution integral. Q_f and $Q_s(t)$ are expressed as

$$Q_f = [I_2]_0[E_{ex} - \Delta H\phi_d]/\phi_d \quad (9)$$

$$Q_s(t) = Q_s\frac{k_{max}t}{1 + k_{max}t} \quad (10)$$

where $[I_2]_0 = (2I_0/I_{sat})[I_2]$ $(=[I]_0/2)$ is the number of parent molecules that dissociate to radicals, $Q_s = \Delta H[I_2]_0$, and $k_{max} = 4k_{rec}[I_2]_0$. ΔH and E_{ex} are the reaction enthalpy and the excitation photon energy, respectively. I_0 and I_{sat} are the laser intensity and the saturation intensity given by $(\sigma^A t_0 \phi_d)^{-1}$, where σ^A is the absorption cross section and t_0 is the pulse duration.

Δn_{pop} is given by

$$\Delta n_{pop}(t) = (\Delta n_{pop}^P/2 + \Delta n_{pop}^R)N_R(t) \quad (11)$$

where Δn_{pop}^P and Δn_{pop}^R denote the changes of the molecular refractive indexes due to the decrease of I_2 and increase of I. $N_R(t)$ is given by

$$N_R(t) = \frac{2[I_2]_0}{1 + k_{max}t} \quad (12)$$

The time profile of Δk_{pop} is given as the same as Δn_{pop}.

Δn_V is given by

$$\Delta n_V(t) = \left(V\frac{\partial n}{\partial V}\Delta V/2\right)N_R(t) = \frac{dn}{dT}\frac{\Delta V}{\alpha_{th}} \quad (13)$$

where α_{th} is the coefficient of the thermal expansion. The reaction volume can be written using the equilibrium constant for the dissociation, $K = [I]^2/[I_2]$, as

$$\Delta V = \kappa_T RT + \Delta V_{conf} = \kappa_T RT - \kappa_T RT\rho_r\left(\frac{\partial \ln K}{\partial \rho_r}\right) \quad (14)$$

where κ_T is the isothermal compressibility of the solvent. The first term is due to the increase of the translational mode by the dissociation, and the second term (ΔV_{conf}), called the configrational volume change,[59] is due to the rearrangement of solvent molecules by the dissociation.

Using the parameters in the above expressions, we can obtain ϕ_d by

$$\phi_d = \frac{E_{ex}}{\Delta H}\frac{Q_s}{Q_s + Q_f} \quad (15)$$

The value of ϕ_d is determined from Q_s and Q_f obtained by a fit of the TG signal to eqs 5−13, and ΔH. The merit of this method lies in the fact that we can determine ϕ_d from a single transient without a reference sample and the absolute laser power profile. On the other hand, the demerit of this method is that we need ΔH beforehand.

The photodissociation quantum yield is also determined by the TG acoustic signal. The density change of the solvent from Δn_{th} and Δn_V creates the acoustic wave if the acoustic transit time over the grating lattice is sufficiently longer than the pulse duration. In our experiment, this time could typically be around 100 ns by making q as small as possible. The acoustic oscillation can be expressed as

$$I_{TG} \propto \left[I_{AC}\left\{1 - \exp(-t/\tau_{AC})\cos\left(\frac{t}{\nu q}\right)\right\} + A\Delta n_{pop}(t)\right]^2 + B\Delta k_{pop}(t)^2 \quad (16)$$

where I_{AC}, A, and B are constants. τ_{AC} is the acoustic damping constant specific to the solvent. In the time range while the acoustic signal is observed, Δn_{pop} and Δk can be assumed to be almost constant. Therefore, when the acoustic signal does not have the population signal, the first acoustic oscillation goes almost to zero.

The intensity of the TG acoustic oscillation I_{AC} is given by

$$I_{AC} \propto \left|\frac{E_{ex} - \phi_d\Delta H}{\rho C_P} + \frac{\phi_d \Delta V}{\alpha_{th}}\right| \quad (17)$$

The first term in eq 17 derives from the fast heat and the second term from the reaction volume, respectively. When the contribution from the reaction volume change is negligible, ϕ_d is determined by using I_{AC} in comparison with the acoustic intensity of the reference sample under the same experimental conditions. Here, the reference sample means the solution of the same absorbance at the excitation wavelength where all the photon energy absorbed by the solute is released as heat within a pulse duration. Then ϕ_d is given by

$$\phi_d = \left(1 - \frac{I_{AC}}{I_{AC}^R}\right)\frac{E_{ex}}{\Delta H} \quad (18)$$

where I_{AC}^R is the TG acoustic intensity of the reference sample.

We also use photoacoustic spectroscopy (PAS)[60,61] to determine ϕ_d for the same purpose as the TG acoustic measurement. In the PAS measurement we measure the intensity of the sound wave formed by the density change, which derives from the fast released heat and the reaction volume change ΔV. The intensity of the PAS signal, I_{PAS}, is given by the same expression as eq 17.[61] Therefore, when the contribution from the reaction volume is negligible, ϕ_d is obtained by

$$\phi_d = \left(1 - \frac{I_{PA}}{I_{PA}^R}\right)\frac{E_{ex}}{\Delta H} \quad (19)$$

where I_{PA}^R denotes the intensity of the reference sample.

3. Experimental Section

The experimental setups of the TG, the TG acoustic, and the PAS measurements were the same as reported previously.[60,62]

In the present study, different types of pulsed lasers were used for excitation at several excitation wavelengths: a Nd:YAG laser (Spectra Physics GCR-170-10, 532 nm, 6−7 ns pulse width), a Nd:YAG laser pumped optical parametric oscillator (OPO) (Spectra-Physics MOPO-710, 490 and 590 nm), an excimer laser pumped dye laser (Lumonics Hyper Dye 400, 440 nm, 15−20 ns). The laser pulse was divided into two pump beams that were crossed in the sample solution at the same time. The beam diameter at the crossing spot was typically 1 mm. After this excitation, the time dependence of the grating was probed by a He−Ne laser (Uniphase, 1137P, 632.8 nm, 7 mW) or diode lasers (SDL, 5311-G1, 802 nm, 100 mW; SDL, 5411-G1, 840 nm, 100 mW). The signal was monitored with a photomultiplier (Hamamatsu R928 for He−Ne laser detection and Hamamatsu R1477 for a diode laser detection) and averaged by a digital oscilloscope (Tektronix TDS-520 or Tektronix 2430A). The static absorption spectra of iodine were measured by a multichannel spectrometer (Otsuka Electronics, MCPD-1000).

Two types of high-pressure optical cells, made of titanium to prevent them from being spoiled by iodine, were used for the measurement. When the pressure was less than 30 MPa, the same cell as reported previously[63] was used. When the pressure was above 30 MPa, a cell made of Ti6Al4V to withstand high pressures up to 350 MPa was used. This cell has an inner volume of about 5 cm^3, a path length of 4 mm, and two optical sapphire windows. The emission from the sapphire windows was eliminated by a cutoff filter. The solvent gases were compressed by a hand-operated hydraulic pressure generator (Nova Swiss). The solutions in the cell were stirred by a magnetic stirrer. The temperature was kept within ±0.1 K by circulating the thermostated water through the cell, and the pressure was measured by a strain gauge (Kyowa PGM 500KH below 30 MPa and Nagano Keiki KH78-161 above 30 MPa). The densities of the fluids were calculated by empirical equations of states.[64] The concentration of iodine in solution was about 1 mM (M ≡ mol dm^{-3}) or less,[65] and in the lower-density region of the fluids ($\rho_r \lesssim 0.4$) the concentration was limited by the solubility.

Gases of Ar (Sumitomo Seika, >99.999%), Kr (Sumitomo Seika, >99.995%), Xe (Iwatani, >99.995%), CO_2 (Sumitomo Seika, >99.99%), C_2H_6 (Sumitomo Seika, >99.0%), N_2O (Sumitomo Seika, >99.9%), and sulfur hexafluoride (SF_6) (Sumitomo Seika, >99.9%) were used as received. Iodine (I_2) (Nacalai Tesque, >99.8%) was used without further purification, which gave the same results as given by that purified by vacuum sublimation. We used phenol blue as a reference. Phenol blue is known to release the absorbed photon energy as the thermal energy within 1 ns.[66] Phenol blue (Aldlich) was purified by recrystallization from ethyl acetate/regloine 1:1 mixture before use. Liquid alkanes of pentane, hexane, heptane (Nacalai Tesque, specially prepared reagent), octane, nonane, decane, and dodecane (Nacalai Tesque, guaranteed reagent) were used without further purification.

4. Results and Discussion

4.1. Liquid Solvents. Typical TG signals for I_2 in hexane at room temperature are shown in Figure 2. We could not detect any TG signal without I_2. The TG signal has an instantaneous rise with the pulse duration and a subsequent slow rise. The former represents the fast heat from the nonradiative decays of excited states and the geminate recombination, and the latter represents the nongeminate recombination. The behavior of the TG signal we measured is almost the same as that reported by Zhu and Harris.[54] The term we want to evaluate from the TG signal is only the thermal grating term. Under our experimental condition, however, the lifetime of the thermal grating ($\tau_{th} = 1/(D_{th}q^2)$) is generally much longer than the inverse of the recombination rate constant. Therefore, the rise profile due to the slow heat is quite similar to the profile of the species grating. This makes the separation of the species grating from the thermal grating difficult. Therefore, it is important in the determination of ϕ_d to know whether the TG signal has a contribution from Δn_{pop}, Δk, and Δn_V.

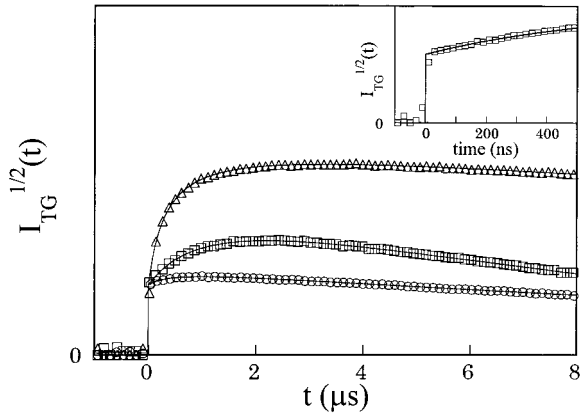

Figure 2. Typical TG signals and fitting curves (solid line) for iodine in hexane (circles) at room temperature: Ar at $\rho_r = 0.4$ and 323 K (squares); CO_2 at $\rho_r = 1.0$ and 323 K (triangles). The inset is the result for the short time scale in Ar after subtraction of the pump scattering.

4.1.1. Contribution to the TG Signal besides the Thermal Grating. The effect of the population grating due to the bleaching of I_2 can be estimated from the analysis of the static absorption spectrum of I_2. By numerical calculation of the refractive index of I_2 from the absorption spectrum in the visible region in hexane, Δn^P_{pop} and Δk^P_{pop} are estimated as $-3.2 \times 10^{-3}[I_2]_0$ and $-7 \times 10^{-4}[I_2]_0$ at 633 nm and as $-1.6 \times 10^{-3}[I_2]_0$ and $-8 \times 10^{-5}[I_2]_0$ at 840 nm, respectively. In this evaluation, we used the Kramers−Kronig relation.[67] On the other hand, $\Delta n_{th}(t=0)$ estimated from eq 8 by assuming the limiting case of $\phi_d = 0$ amounts to $-1.1 \times 10^{-1}\Delta N$,[68,69] where ΔN is the number of iodine molecule that absorbs the photon. Therefore, the contributions of Δn_{pop} and Δk_{pop} due to the ground-state bleach are less than 3% and 1% at 633 nm, respectively, which will be smaller at 840 nm. Our estimation is almost consistent with that by Zhu and Harris[54] and suggests that the contribution of the population grating is negligibly small. Zhu and Harris have also evaluated the contribution of the excited-state absorption and found that it makes a negligible contribution.

To make a further verification experimentally, we measured the probe wavelength dependence of the TG signal. If Δn_{pop} and Δk cannot be neglected, the TG signal is dependent on the wavelength of the probe beam. We have measured the TG signal at several probe wavelengths of 633, 802, and 840 nm in alkanes and could not detect any meaning difference in the value of Q_s/Q_f obtained by the signal fit with only the thermal grating term (see the result of ϕ_d in Figure 4). In the fitting, we used $D_{th}q^2$ determined by the reference signal (phenol blue in the same solvent).[70]

We also measured the TG acoustic signal in hexane, shown in Figure 3. As mentioned in section 2, if there is a contribution from Δn_{pop} or Δk, the acoustic oscillation does not reach the baseline. It was found that the first bottom of the oscillation almost reaches the baseline. This fact supports that the contribution of Δn_{pop} and Δk is negligible.

The next problem is the contribution of Δn_V. The value of ϕ_d is estimated to be larger if the reaction volume change for

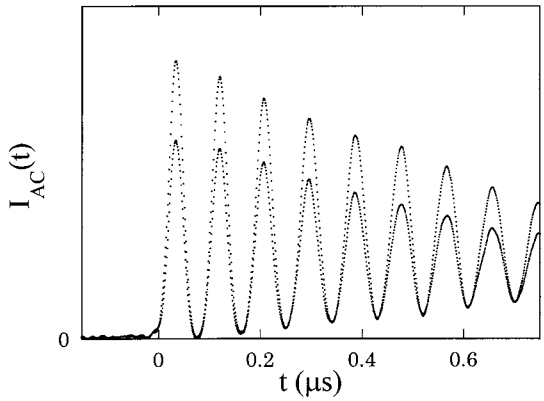

Figure 3. TG acoustic signal for iodine (smaller intensity) and phenol blue (larger intensity) in hexane at room temperature.

the dissociation ΔV is negative and smaller if positive. This is because Δn_{th} is always negative and Δn_V is also negative if ΔV is positive. The ratio between the intensity of the volume grating to the thermal grating is given by

$$\frac{\Delta n_V(0)}{Q_s + Q_f} = \frac{\rho C_p \phi_d}{h\nu \alpha_{th}} \Delta V \qquad (20)$$

Using eq 20, we can estimate ϕ_d for a given ΔV by a fit of the TG signal. Unfortunately, ΔV for the iodine dissociation has not been determined. ΔV for the dissociation of molecule of similar size in liquid is generally a few tens of cm^3/mol. For example, ΔV for the dissociation of 2-methyl-2-nitrosopropane in carbon tetrachloride has been estimated as about 40 cm^3 mol^{-1}.[71] In the case of heptane, the change of ϕ_d is 0.04 for ΔV of 40 cm^3 mol^{-1}. This change is comparable to or a little larger than the experimental error. Therefore, our results in liquids have an ambiguity of this order. We conclude that the TG signal can be analyzed with only the thermal grating term in liquid solvents.

4.1.2. Verification of the Simplified Analysis. To show that our simplified analysis is appropriate, we measured the TG signal at various values of q. In our simplified simulation (eqs 5−13), the parameter q appears only in the decay constant, although the exact expression has the parameter of q in the slow rise term. The exact expression of the diffraction efficiency η is[54]

$$\eta = [Ag_1(t) \exp(-D_{th}q^2t) + B \exp(-D_{th}q^2t)]^2 \qquad (21)$$

$$g_1(t) = \frac{2q}{\pi}\int_0^{\pi/q} \frac{k_{max}[1 - \exp(1 - I(x)/I_{sat})]}{\{1 + k_{max}[1 - \exp(1 - I(x)/I_{sat})]t\}^2} \times \cos(qx)\, dx \qquad (22)$$

where we used the same notation as in ref 54. We measured the TG signal at various q^2 from 0.25 to 0.75 μm^{-2} but could not detect meaningful q^2 dependence. Indeed, even if we analyze the TG signal with the rigorous expressions of eqs 21 and 22, both results coincide with each other within an error of 5%.

Another problem is an effect of the saturation. To check this effect, we measured the excitation power dependence and the concentration dependence of the sample solution. The excitation power was varied from 2 to 15 μJ/pulse with a spot size of ca. 0.008 cm^2 and the concentration was varied from 0.1 to 1.0 of the optical density at 532 nm with a 1 cm path length. We could not detect any meaningful power and concentration dependence, and the estimated values of ϕ_d coincide with each other within an error of 8% in both cases. In fact the laser intensity (<0.3 MW cm^{-2}) is much lower than the saturation intensity (6 MW cm^{-2}) evaluated by Zhu and Harris.[54]

TABLE 1: Comparison of the Photodissociation Quantum Yields in Hexane and Heptane Determined by Several Experimental Methods

	excitation wavelength (nm)	hexane	heptane	ref
transient grating	532	0.26 ± 0.03	0.24 ± 0.03	
photoacoustic	532	0.22 ± 0.03		
TG acoustic	532	0.26 ± 0.05		
photothermal grating	532	0.25 ± 0.03	0.19 ± 0.02	54
transient absorption	590		0.15 ± 0.01	29
transient absorption	492		0.23 ± 0.01	36
transient absorption	532	0.37		23
radical trap	546.1	0.46 ± 0.07		4

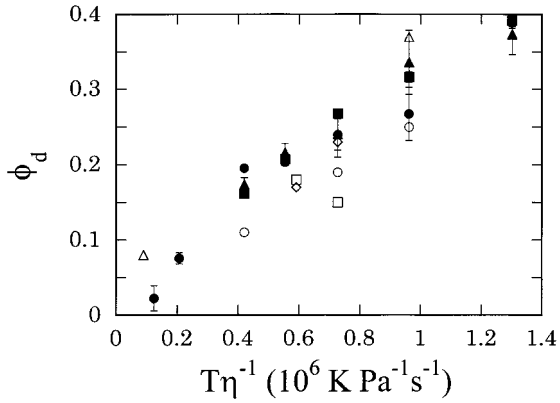

Figure 4. Viscosity dependence of ϕ_d in various liquid alkane solvents obtained by the TG method at different probe wavelengths: filled circles, 633 nm; filled squares, 802 nm; filled triangles, 840 nm. From left to the right, the solvents are dodecane, decane, nonane, octane, heptane, hexane, and pentane. The values from the literature are also indicated: open circles from ref 54 (nonane, heptane, hexane); open squares from ref 29 (isooctane, heptane); open rhombuses from ref 36 (isooctane, heptane); open triangle from ref 23 (hexadecane, hexane).

To make sure of our simplified analysis, we have also checked the conservation of the total heat. The sum of the intensities of the fast and the slow rises in the sample solution ($Q_s + Q_f$) obtained by the fitting has to be equal to the intensity of the TG signal (Q_{ref}) for the reference sample. The averaged ratio between ($Q_s + Q_f$) in the sample solution to (Q_{ref}) in the reference sample is obtained as 1.02 ± 0.04.

4.1.3. Photodissociation Quantum Yield in Liquids. From the above discussions, we believe that the measurement and the analysis are appropriate. We show ϕ_d in heptane and hexane obtained by the TG, the TG acoustic, and the PAS and from some other literature (the photothermal grating spectroscopy,[54] the transient absorption,[23,29,36] and the radical trapping[4] experiments) in Table 1. We also show the results in several alkanes in Figure 4. In the calculation of ϕ_d, ΔH was assumed to be constant as 36 kcal mol^{-1}, which was obtained in gaseous phase.[72] Although the solvation may change the reaction enthalpy, the effect is considered to be small, as is represented by the small solvent effect on the absorption spectrum as will be discussed later. Zhu and Harris estimated ΔH as 31 kcal mol^{-1} in hexane, 34 kcal mol^{-1} in heptane, and 36 kcal mol^{-1} in nonane.[54] The difference of 3 kcal/mol results in the different estimation of ϕ_d as about 10% in the case of hexane. Our results measured by the TG, the TG acoustic, and the PAS measurements are very similar. It can be said that the radical trapping method overestimates the photodissociation quantum yields. As is shown in Figure 4, ϕ_d decreases with increasing the solvent

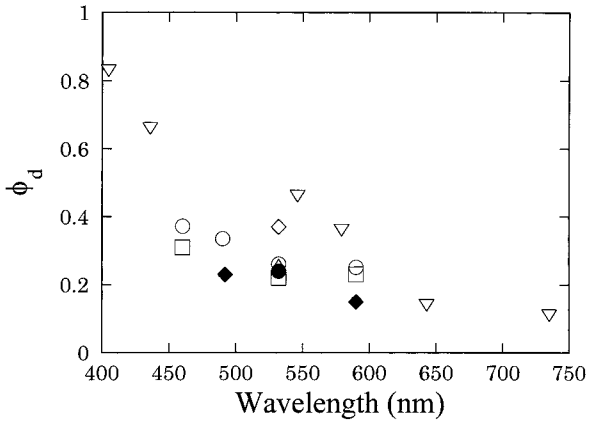

Figure 5. Excitation wavelength dependence of ϕ_d for iodine in hexane (open symbols) and heptane (filled symbols) at room temperature, estimated by TG (circles), PAS (squares), TG acoustic (triangles), radical trapping (inverse triangle),[4] and TA (rhombuses, 490 nm,[36] 532 nm,[23] 590 nm[29]).

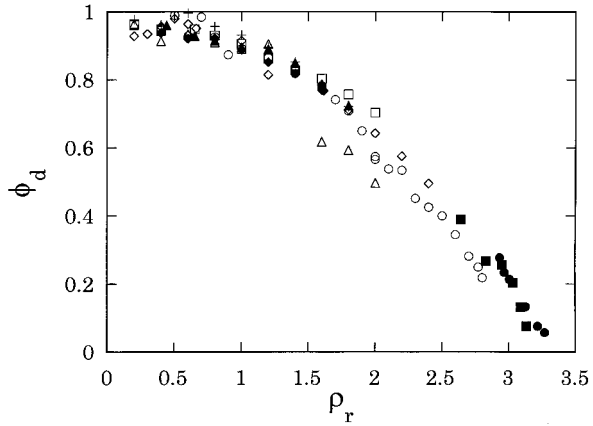

Figure 6. Photodissociation quantum yields estimated by the TG signal with only thermal grating term for iodine in C_7H_{16} (filled circles) at 298 K, Ar (open rhombuses) at 323 K, Kr (filled rhombuses) at 293 K, Xe (crosses) at 323 K, CO_2 (open circles) at 323 K, C_2H_6 (open squares) at 323 K, SF_6 (open triangles) at 333 K, N_2O (filled triangles) at 323 K, and alkanes (filled squares) at room temperature.

viscosity, consistent with other values determined by the different methods, although there is a scattering of data depending on the different experimental methods. The viscosity dependence will be discussed in the section 4.2.3.

Noyes et al. reported significant wavelength dependence of ϕ_d.[4] In constrast, Troe et al. reported that no significant wavelength dependence was observed above the excitation wavelength of 581 nm.[30] Before the discussion of ϕ_d over a wide solvent density region, we mention the excitation wavelength dependence of ϕ_d measured by the TG method. In Figure 5, we show the excitation photon energy dependence in hexane and heptane determined by this work together with the values in the literature. As is shown in the figure, we did not detect a large dependence on the excitation wavelength as was reported by Noyes et al., although a similar tendency (with increasing excitation energy, ϕ_d increases) was observed. The result suggests that the simple hydrodynamic model cannot be applicable to the photodissociation dynamics partly because of the complexity of the reaction dynamics of iodine. We consider that the excess energy of the separating atoms is more effectively lost as heat than is expected from the hydrodynamic prediction.

4.2. Low-, Medium-, and High-Density Fluids. *4.2.1. Analysis with Only the Thermal Grating Term*. In this section, we will discuss the results in low-, medium-, and high-density fluids. Typical TG signals for Ar (squares) at $\rho_r = 0.4$ and 323 K, and CO_2 (triangles) at $\rho_r = 1.0$ and 323 K are also shown in Figure 2. It is apparent that the slow-rise part relative to the fast-rise part in fluids is much larger than those in liquid solvents. It is useful to see what kind of solvent density dependence is extracted by fitting the TG signal only with the thermal grating term, since in the liquid phase the thermal grating is the only main contribution to the TG signal. In such an analysis, we fitted the signal by eqs 9 and 12, assuming that k_{max}, Q_f, Q_s, and $D_{th}q^2$ are adjustable parameters. The obtained D_{th} from the TG signal showed the density dependence, as is expected from the literature values of the thermal conductivity, C_P, and ρ. Although we varied q^2 from 0.25 to 0.75 μm^{-2}, we could detect no meaningful q^2 dependence on the estimated ratio Q_s/Q_f. We also measured the excitation power dependence of the TG signal in CO_2 at $\rho_r = 0.6$ and $\rho_r = 1.0$ at 323 K and could not detect a meaningful power dependence of the ratio Q_s/Q_f from 4 to 16 μJ with a spot diameter of ca. 1 mm.

Figure 6 shows ϕ_d obtained by the TG fitting with only the thermal grating term. They are very different from those reported by the transient absorption experiment, especially in the low-density and the medium-density regions. In the transient absorption experiment, the quantum yields are extremely low in CO_2, C_2H_6, N_2O, and so on. However, the quantum yields by the TG method hardly depend on the solvent species. The difference may be ascribed to the effects of contributions other than the thermal grating. We now consider the possible existence of the contribution of the population grating and the volume grating.

4.2.2. Contributions besides the Thermal Grating. The amplitude of the population grating can be roughly estimated from the absorption spectrum as is done in the case of liquids. The peak of the visible absorption spectrum of iodine is around 520 nm at 298.15 K for the vapor of iodine.[73] It shifts to 522.5 nm at 313.5 K and 13.3 MPa in Xe[73] and from 522 nm at 0.1 MPa to 517 nm at 500 MPa in C_7H_{16}.[30] The shape of the absorption spectrum and the integrated absorption cross section do not change.[30] Nearly the same behavior is found in other solvents.[30] This indicates that the absorption spectrum is almost the same as in the liquid alkanes and that the orders of Δn^P_{pop} and Δk^P_{pop} are similar to those in hexane. The value of Δn_{th} is dependent on the solvent density, since parameters such as C_P and dn/dT are strongly dependent on the solvent density. By assuming that dn/dT is given by $(\partial n/\partial \rho)(\partial \rho/\partial T)$, we evaluated the order of Δn_{th} in CO_2 at 320 K from the reported values of n,[74] C_P,[75] and α_T evaluated by the equation of state.[64] According to the calculation, $\Delta n_{th} \approx 3 \times 10^{-1}\Delta N$ at $\rho_r \approx 0.3$, $4 \times 10^{-1}\Delta N$ at $\rho_r \approx 1$, and $1 \times 10^{-1}\Delta N$ at $\rho_r \approx 2$. Therefore, the contribution of the population grating due to I_2 is also expected to be negligible in fluids over a wide density region.

The effect of the excited-state absorption such as the A/A′ state is somewhat subtle. If the lifetime of the state is less than 1 ns, we can safely neglect the contribution. On the other hand, if the lifetime is between 10 ns and a few hundred nanoseconds, the population grating signal may appear as a sharp spike in the TG signal. To test this possibility, we have measured several TG signals at a very early time after excitation in Ar and C_2H_6. The result in Ar at $\rho_r = 0.3$ is depicted in the inset of Figure 2. In this plot, the scattering of the pump beam measured under the same experimental condition is subtracted from the TG signal. As is shown in the figure, we could not detect a spike. The solid line in the figure is the fitting line determined at the longer time range where we mainly made the measurement, and the fitting curve reproduces the signal even on the short time scale. If the lifetime is more than a few hundred nanoseconds,

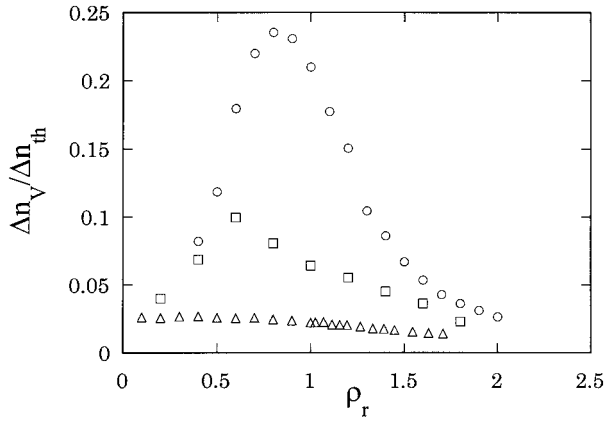

Figure 7. Ratio $\Delta n_V/\Delta n_{th}$ estimated in CO_2 (circles), Xe (squares), and Ar (triangles) at 323 K.

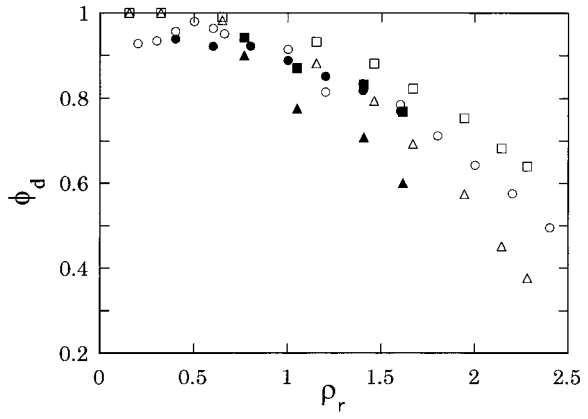

Figure 8. Photodissociation quantum yields in Ar (open circles) and Kr (filled circles) estimated by the TG method in Ar (open triangles) and Kr (filled triangles) determined by Zewail et al.[15] and in Ar (open squares) and Kr (filled squares) estimated by using the TG data as the reference.

we cannot separate the contribution from the slow-rising part because of the nongeminate recombination. However, we consider that such a situation is improbable from the experimental studies made until now.[57,58] We have also experimentally demonstrated that there is little probe wavelength dependence of the estimated Q_s/Q_f at the wavelength 633 and 840 nm in CO_2 from $\rho_r = 0.4$ to $\rho_r = 1.8$ and C_2H_6 from $\rho_r = 0.4$ to $\rho_r = 2.0$. These facts mean the absence of the contribution of the population grating.

Next we consider the effect of Δn_V, which may be different from that in liquid solvents, since the reaction volume is strongly dependent on the solvent density. In the medium-density fluids, the reaction volume may be very large because of the large compressibility of the solvent. In fact, it was reported that the ΔV_{conf} in eq 14 for the dissociation reaction of 2-methyl-2-nitrosopropane has a large negative value in the medium-density region.[76−78] Since the reaction volume of iodine has not been known until now, we attempt to estimate the reaction volume by $\kappa_T RT$, which determines the magnitude of the reaction volume in the medium-density region (see eq 14). We calculated Δn_V, assuming $\phi_d = 1$, and Δn_{th}, assuming $\phi_d = 0$. The results are shown in Figure 7. The contribution of Δn_V relative to Δn_{th} is small in Ar (triangle) and Kr (not in the figure), which is far from the critical point. The intensity is less than 3% in Ar and 4% in Kr relative to the intensity of Δn_{th}. Therefore, Δn_V is small enough to be neglected in the cases of Ar and Kr. In C_7H_{16}, we measured the density region higher than $\rho_r = 2.9$, where the effect of Δn_V is small. Even in CO_2, Δn_V is considered to be sufficiently small at the low and high densities. On the other hand, Δn_V may be large at a medium density of CO_2. Similar behavior is expected for the cases of C_2H_6, N_2O, SF_6, and Xe whose critical temperatures are close to the temperature in this work. In the following, we will separately discuss the experimental results for two cases depending on whether Δn_V can be neglected or not.

4.2.3. In Ar, Kr, and C_7H_{16}. In Ar, Kr, and C_7H_{16}, Δn_V is small enough to be neglected in all the density regions measured, and the analysis of the TG signal should give reliable values of ϕ_d. Figure 8 shows the results in Ar (open circles) and Kr (filled circle) with those in Ar (open triangles) and Kr (filled triangles) reported by Zewail et al.[15] Our results are different in the high-density region, although they are in good agreement in the low- and the medium-density regions. They estimated the geminate recombination yield ϕ_{rec} ($=1 - \phi_d$) by using a value a_{rec} that is the intensity of the signal of the excited A′ state due to the geminate recombination after the excitation of iodine at 620 nm. They considered that the value of a_{rec} is proportional to ϕ_{rec} and calculated ϕ_{rec} at any state with respect to the standard state (Kr at 40 MPa). They used the value of ϕ_{rec} as 0.4 for the standard state, which was determined by a transient absorption experiment.[36] Therefore, if ϕ_{rec} at the standard state is changed, ϕ_{rec} at any state will be different. In Figure 8, we also show the results in Ar (open squares) and Kr (filled squares) that are obtained by using the value of $\phi_{rec} = 0.23$ for the standard state, which is determined in the present work. The agreement with the TG results is much better, although there are still some differences in the case of Ar. We are not sure of the reason for the difference, but several explanations may be possible; the density dependence of the reaction enthalpy that was neglected in the TG analysis or the solvent dependence of the branching ratio on different electronic states that was neglected in the transient absorption analysis. The excitation wavelength dependence of the quantum yield may be another reason for the difference.

In the later part of this section, we will discuss the density dependence of ϕ_d from the TG method on the basis of the diffusion model. We show ϕ_d in C_7H_{16} obtained by the TG method (circle) and by the transient absorption (square) in Figure 9 against the diffusion coefficient of the iodine atom. The diffusion coefficient is estimated from the viscosity η via an extension of the Stokes−Einstein relation to low pressure as is done by Troe et al.[30,79] Explicitly,

$$\frac{kT}{\eta D} \cong 3\pi\sigma_I\left\{1 - \exp\left(-\frac{[M]}{[M]_c}\right)\right\} \tag{23}$$

where σ_I denotes the Lennard-Jones diameter of free iodine atoms and $[M]_c$ the critical density of the solvent. The value $\sigma_I = 4.320$ Å is used.[30] Our results give a dependence on D^{-1} similar to that of the transient absorption, although our values are generally larger.

Now we consider the diffusion model eq 2 to interpret the density dependence of ϕ_d. In the previous work,[30] k_{rec}^g was assumed to be proportional to D^{-1}, and the proportional constant was different between the low- and high-density regions. We assume that k_{rec}^g depends on the diffusion coefficient D as $k_{rec}^g \propto D^{-b}$. Then eq 2 is re-expressed as

$$\phi_d = \frac{1}{1 + aD^{-(1+b)}} \tag{24}$$

where a and b are constants. We fitted ϕ_d in C_7H_{16} from the TG method and the transient absorption with eq 24. Although

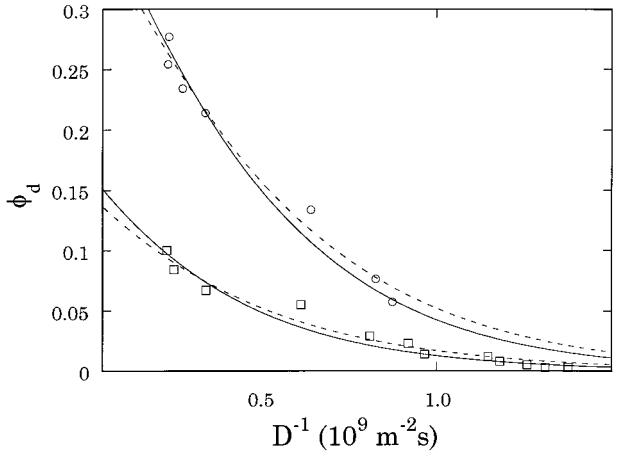

Figure 9. Photodissociation quantum yields estimated in C_7H_{16} at 298 K by the TG method (circles) and the transient absorption[29] (squares). Solid curves are the best fit to eq 30, and dashed curves are the best fit to eq 30 with $b = 1$.

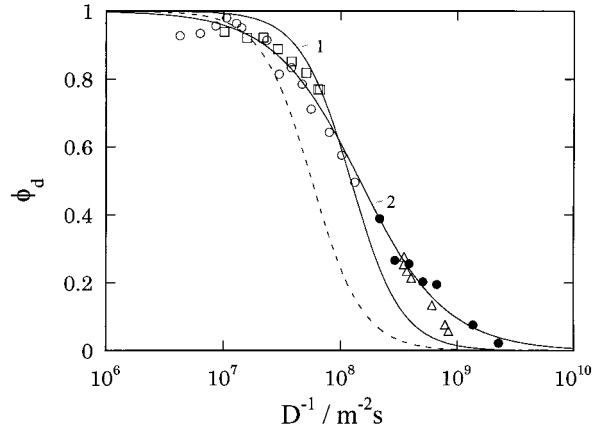

Figure 10. Photodissociation quantum yields by TG for iodine in Ar at 323 K (open circles), Kr at 293 K (open squares), C_7H_{16} at 298 K (open triangles), and alkanes at room temperature (filled circles). The solid curve 1 is the fit to eq 25 assuming $b = 1$ for all of these quantum yields. The solid curve 2 is the best fit to eq 25. The dashed curve is values calculated from eq 2 with k_{rec}^g for the gas phase from eq 3.

it seems that eq 24 with $b = 1$ well reproduces the experimental ϕ_d (dashed curves), the best fits (solid curves) give $b = 0.7$ in both cases.

We also tried to fit ϕ_d from the TG method in all the density regions measured in Ar and Kr with eq 24. Figure 10 shows the fits of ϕ_d, in which the solid curve 1 shows the fit to eq 24 assuming $b = 1$, the solid curve 2 shows the best fit to eq 24, and the dashed curve shows calculated values of ϕ_d by eq 2 with k_{rec}^g in the gas phase of Ar assuming eq 3. It has been proved that the linear relationship of k_{rec}^g with D^{-1} holds up to $D^{-1} \approx 10^7$ m^{-2} s in Ar.[26] The experimentally obtained ϕ_d lies around the dashed line in these density regions. Above 10^7 m^{-2} s, the deviation of ϕ_d from the gas-phase prediction is evident. The best fit to eq 24 gives $b = 0.25$. It is surprising that ϕ_d for all cases of solvents are on the same curve, although k_{rec}^g depends on the species of the solvent in the gaseous phase.[26]

As is shown in the figure, the diffusion model is successful in the interpretation of the density dependence of ϕ_d, although several modifications are required to get a quantitative agreement. There are several reasons why b is not equal to 1. First, k_{rec}^g is not proportional to D^{-1} in the high-density region. k_{rec}^g is considered to correspond to the energy relaxation rate from the encounter complex. In the case of iodine, the proportionality

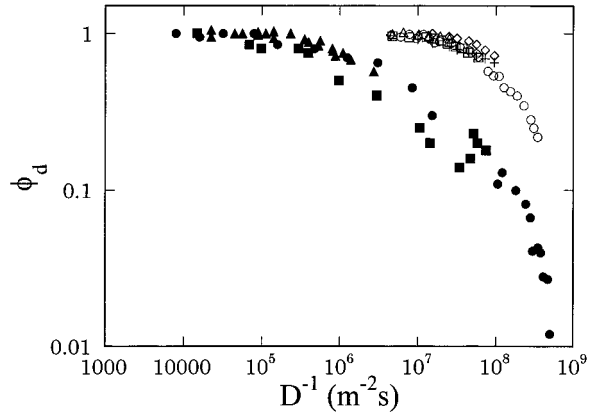

Figure 11. Photodissociation quantum yields in CO_2 (open circles), C_2H_6 (open squares), N_2O (open triangles), Xe (open rhombuses) at 323 K by the TG method and CO_2(filled circles), C_2H_6 (filled squares), N_2O (filled triangles), and Xe (crosses) by transient absorption.[27,30,36]

of the vibrational energy relaxation rate to the diffusion coefficient holds only under a limited condition. In general, the dependence of the energy relaxation rate on the solvent density is smaller than the dependence of the diffusion coefficient.[80−82] Therefore, $k_{rec}^g \propto D^{-b}$ with $b < 1$ is expected. In relation to this, the constant a also should be dependent on the solvent density as was shown by Troe's group.[30] This is because k_{rec}^g obeys $k_{rec}^g \propto D^{-1}$ in the low-density region, while k_{rec}^g should obey $k_{rec}^g \propto D^{-b}$ ($b < 1$) in the medium- and the high-density regions. Although the density dependence of the constant a will modify the constant b, we consider constant b should still be less than 1.

Finally, the contribution of the primary geminate recombination should be included. The primary geminate recombination is not considered in the diffusion model. Therefore, ϕ_d has to be expressed as eq 2 multiplied by a fraction of the secondary and nongeminate recombination. Zewail et al. suggested that a nonnegligible contribution of the primary geminate recombination exists in the case of rare gases.[15] These three factors mentioned above should be included to get a quantitative agreement with the diffusion model.

4.2.4. In CO_2, C_2H_6, N_2O, Xe, and SF_6. The quantum yields in CO_2, C_2H_6, and N_2O obtained by the transient absorption are much smaller than in rare gases, which is explained by the cluster model,[30,36] although those in Xe and SF_6 by the transient absorption are the same as in Ar and Kr.[36] However, our results are quite different quantitatively from the results by the transient absorption in CO_2, C_2H_6, and N_2O. In Figure 11, we compare the results by the TG method with the results by the transient absorption method,[27,30,36] where the results of the TG method are estimated by the analysis with only the thermal grating term. Since the viscosity of SF_6 is not available, we do not include the results of SF_6 in the figure. ϕ_d values obtained by the transient absorption for SF_6 are also the same as in rare gases. The estimated values of ϕ_d in these fluids by the TG method are very similar to those in the rare gases.

In these fluids, as is mentioned in section 4.2.2, the contribution from the reaction volume may not be negligible because of the large isothermal compressibility of the solvent in the medium-density region. It is possible that ΔV contributes to the TG signal significantly to make ϕ_d from the TG method artificially larger. However, we believe that this possibility is not probable because of the following reason. If we calculate ΔV from the fitting of the TG signal with the reported ϕ_d, ΔV should be a very large negative value and should depend on

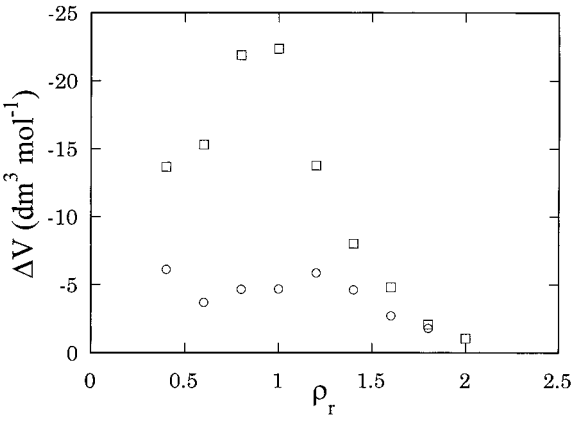

Figure 12. Estimated ΔV to agree with results from transient absorption in CO_2 (circles) and C_2H_6 (squares).

the density very much, as is shown in Figure 12. In this signal simulation, the reaction enthalpy ΔH is assumed to be constant. However, the large ΔV should change ΔH by

$$\Delta H = \Delta U + \frac{\alpha_{th}}{\kappa_T} T \Delta V \tag{25}$$

where ΔU is the internal energy change. Therefore, the large negative ΔV leads to smaller ΔH according to eq 25, if ΔU is constant. Generally, ΔU has a tendency to become small with a decrease of ΔV, since a negative ΔV means that the iodine atom is more solvated than the iodine molecule. Given this smaller ΔH, ϕ_d from the TG signal becomes larger. Consequently, we have to assume a larger negative value of ΔV in order to reduce ϕ_d. We have tried to estimate the contribution of ΔV in order that ϕ_d will agree with the results by the transient absorption and that eq 25 will be satisfied. The values of ΔV by this estimation are much more negative than those shown in Figure 12, and the values of ΔH are negative. The negative ΔH makes the iodine molecules the separated atom automatically, but such a phenomenon was not observed during the experiment.

We have tried to estimate the lower-limit value of ϕ_d by the TG measurement in the limiting case of $\Delta H \rightarrow 0$. The limiting values are often close to the values estimated by assuming only the thermal grating in the medium-density region. For example, for $\rho_r = 1.2$ of CO_2, this minimum value is 0.7, while the value with the assumption of $\Delta V = 0$ is 0.86. This fact indicates that the contribution of the volume grating does not strongly influence the estimation of ϕ_d. Consequently, we believe that the photodissociation quantum yields in the low- and medium-density fluids are close to the values in rare gases.

The fact that in Xe and SF_6 we have a density dependence of ϕ_d similar to that by the transient absorption method also suggests that the difference observed in CO_2, C_2H_6, and so on cannot be explained by the volume grating contribution. Since the magnitude of $\kappa_T RT$ is similar to each other, the effect of the volume grating in Xe and SF_6 is expected to be similar to that in CO_2, C_2H_6, and so on, if the solute−solvent interactions are not so different from one another. If the solute−solvent interactions are quite different from one another in these solvent fluids, it is possible that the contributions of the volume grating are different owing to the different density dependence of the equilibrium constant for the dissociation of I_2 (see eq 14).

To test this possibility, we will estimate the strength of the interaction between iodine and the solvent molecule from the solubility data. The logarithm of the solubility relative to the vapor pressure of pure solute at a given temperature is related to the second virial coefficient between solute and solvent as[83]

$$\ln \frac{C}{C_0} = (V_S - 2B_{12})\rho + D\rho^2 + ... \tag{26}$$

where C and C_0 are the concentrations of the solute at the solvent density ρ and at the vapor pressure, respectively, V_S is the volume in the solid phase, and B_{12} stands for the second virial coefficient of the mixture. B_{12} is related to the intermolecular potential $V(\mathbf{r})$ as[84]

$$B_{12} = -\frac{N_A}{2}\int_0^\infty \left(\exp\left(-\frac{V(\mathbf{r})}{kT}\right) - 1\right) d\mathbf{r} \tag{27}$$

Since the interaction between iodine and solvent is not isotropic, the exact estimation of the potential from only B_{12} is impossible. To extract the typical strength of the attractive interaction (or orientationally averaged interaction), we simply assumed the Lennard-Jones (LJ) potential as $V(\mathbf{r})$ and extracted the LJ parameters from this equation. By using the available solubility data,[73,85,86] we obtained $B_{12} = -250$ cm^3/mol in CO_2 at 323.2 K and $B_{12} = -380$ cm^3/mol in Xe at 313.5 K.[87] These values and eq 27 give the value of ϵ/k for the LJ potential as 293 K in CO_2 and 352 K in Xe if we employ the core parameter σ listed in Table 2. These values are very close to those estimated from Berthelot's law (see Table 2).[88] This suggests that the orientationally averaged interaction between CO_2 and iodine is similar to that between iodine and Xe. Therefore, the effect of the volume grating is expected to be similar to each other in these solvent fluids.

TABLE 2: Lennard-Jones Parameters

	ϵ/k (K)	ϵ/k (K)	σ (Å)
CO_2-CO_2	195[a]		3.9[a]
Xe−Xe	231[a]		4.1[a]
I_2-I_2	474[a]		5.2[a]
CO_2-I_2	304[b]	293[c]	4.55[d]
Xe−I_2	331[b]	352[c]	4.65[d]

[a] Reference 82. [b] Estimated value from Berthelot's law. [c] Estimated value from the second virial coefficient (this work). [d] Estimated value from Lorentz's law.

It is also noted that the caging effect on ϕ_d could not be observed for the 1:1 complex between solute and solvent in the case of the I_2^- cluster. Lineberger et al. found the fraction of the photodissociation of $I_2^-(CO_2)_n$ to be unity in the case of $n < 6$.[89] The excitation wavelength for their experiment is 720 nm, which corresponds to an excess energy of 5800 cm^{-1}. The excess energy is almost similar to that of the present case. The results suggest that the small size of the cluster does not quench the dissociation.

To evaluate the average cluster size in the case of iodine in CO_2 and Xe, we have evaluated the coordination number around the iodine molecule on the basis of the intermolecular potential determined above. We have calculated the solute−solvent radial distribution function $g_{SX}(r)$ using the PY approximation for the Lennard-Jones fluid, where the subscripts S and X mean the solvent and iodine, respectively. We have calculated $g_{SX}(r)$ at $T^* (=kT/\epsilon_{SS}) = 1.4$ from $\rho^* (=\rho\sigma_S^3) = 0$ to $\rho^* = 0.8$. The critical temperature and the critical density of the LJ fluid are 1.32 and 0.31 in the reduced unit, respectively.[90] The calculation procedure is given in ref 91. We have calculated three cases (a) $\epsilon_{SX} = \epsilon_{SS}$, (b)$\epsilon_{SX} = 1.5\epsilon_{SS}$, and (c) $\epsilon_{SX} = 2\epsilon_{SS}$. In all cases $\sigma_X = 1.3\sigma_S$. Case b is close to the experimental condition for iodine in Xe or iodine in CO_2 according to the potential

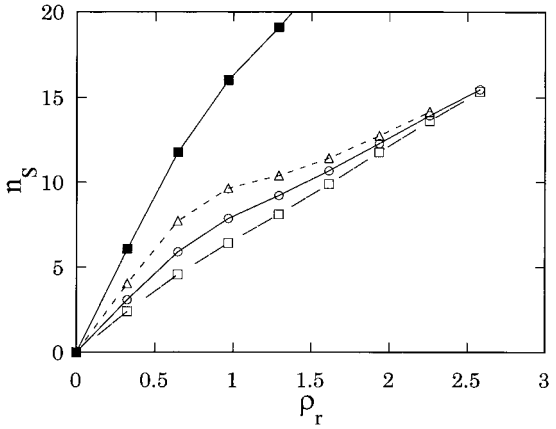

Figure 13. Coordination number around the solute molecule against solvent density at the reduced temperature $T^* = 1.4$ with several values of ϵ_{SX}: $\epsilon_{SX} = \epsilon_{SS}$ (open squares), $\epsilon_{SX} = 1.5\epsilon_{SS}$ (open circles), and $\epsilon_{SX} = 2.0\epsilon_{SS}$ (open triangles). $g_{SX}(r)$ is integrated to $1.65\sigma_S$ for the above three cases and to $2.15\sigma_S$ with $\epsilon_{SX} = 1.5\epsilon_{SS}$ (filled squares).

parameters in Table 2. The coordination numbers calculated by integrating $g_{SX}(r)$ within the first solvation shell ($r = 1.65\sigma_S$) are shown in Figure 13. The density that gives $n = 6$ is around $\rho_r = 0.5$, and the results cannot be very different even if the interaction is stronger, or the distance at which the solvent influences the dissociation is assumed to be longer. According to this calculation, there are only a small number of solvent molecules around the iodine in the lower-density fluid, which does not affect ϕ_d of I_2^-. Therefore, to explain the decrease of ϕ_d observed in the TA method, we have to invoke the factor that is neglected in the above discussion, such as the orientational effect; e.g., the special solvation site of iodine occupied by carbon dioxide may quite effectively suppress the photodissociation, which is not the case with I_2^-. Anyway at present, we could not find a reasonable explanation for the discrepancy between the TG method and the TA method.

5. Conclusion

We have extended and simplified the analysis proposed by Zhu and Harris to measure ϕ_d of iodine in various solvent species and at different densities. We have demonstrated that the contributions of the population grating due to the ground and the excited states are negligible. In fluids where the contribution of the volume grating is negligible such as Ar, Kr, and C_7H_{16}, we have determined ϕ_d at various solvent densities. In C_7H_{16}, the solvent density dependence of ϕ_d is qualitatively similar to the results measured by the transient absorption, although quantitatively different. In Ar and Kr, the solvent density dependence of ϕ_d is similar to the results of Zewail et al. We applied the diffusion model to interpret the density dependence of ϕ_d. Although the diffusion model works well qualitatively, our results suggest that several modifications are required to get a quantitative agreement.

The results in fluids near the critical temperature are controversial. In CO_2, C_2H_6, and N_2O, ϕ_d obtained by a fit of the TG signal with only the thermal grating term is very different from those by the transient absorption, while ϕ_d in Xe and SF_6 estimated by the TG signal is in agreement with ϕ_d by the transient absorption. Although the contribution of the volume grating may decrease ϕ_d, the effect is estimated to be not so large to make the TG results agree with the results by the transient absorption. We have also demonstrated that no specific interaction exist between I_2 and CO_2 from the examination of the density dependence of the solubility.

At present we do not have any explanation of the discrepancy between our results and those by the transient absorption. However, we consider that the cluster model proposed by Troe's group requires quite a special mechanism for quenching, even if their results are correct. The estimated coordination number around the iodine molecule based on the potential determined by the solubility suggests that there is no meaningful difference between the cases of Xe and CO_2 and that a large number cluster, which affects ϕ_d in the case of $I_2(CO_2)^-$, exists above $\rho_r = 0.5$. Further studies will be required to resolve the problem.

Acknowledgment. We thank Mr. F. Amita (Kyoto University) for constructing the optical cell for the high-pressure measurement. This work is supported by a Research Grant-in-Aid from the Ministry of Education, Science, and Culture (No. 07640673) and by CREST (Core Research for Evolutional Science and Technology) of Japan Science and Technology Corporation (JST).

References and Notes

(1) Franck, J.; Rabinowitch, E. *Trans. Faraday. Soc.* **1934**, *30*, 120.
(2) Zimerman, J.; Noyes, R. M. *J. Chem. Phys.* **1950**, *18*, 658.
(3) Booth, D.; Noyes, R. M. *J. Am. Chem. Soc.* **1960**, *82*, 1868.
(4) Meadows, L. F.; Noyes, R. M. *J. Am. Chem. Soc.* **1960**, *82*, 1872.
(5) Tellinghuisen, J. *J. Chem. Phys.* **1982**, *76*, 4736.
(6) Potter, E. D.; Liu, Q.; Zewail, A. H. *Chem. Phys. Lett.* **1992**, *200*, 605.
(7) Liu, Q.; Wang, J. K.; Zewail, A. H. *Nature* **1993**, *364*, 427.
(8) Wang, J. K.; Liu, Q.; Zewail, A. H. *J. Phys. Chem.* **1995**, *99*, 11309.
(9) Bowman, R. M.; Dantus, M.; Zewail, A. H. *Chem. Phys. Lett.* **1989**, *161*, 279.
(10) Yan, Y.; Whitnell, R. M.; Wilson, K. R.; Zewail, A. H. *Chem. Phys. Lett.* **1992**, *193*, 402.
(11) Wan, C.; Gupta, M.; Baskin, J. S.; Kim, Z. H.; Zewail, A. H. *J. Chem. Phys.* **1997**, *106*, 4353.
(12) Lineau, C.; Williamson, J. C.; Zewail, A. H. *Chem. Phys. Lett.* **1993**, *213*, 289.
(13) Lienau, C.; Zewail, A. H. *Chem. Phys. Lett.* **1994**, *222*, 224.
(14) Lienau, C.; Zewail, A. H. *J. Chim. Phys.* **1995**, *92*, 566.
(15) Lienau, C.; Zewail, A. H. *J. Chem. Phys.* **1996**, *100*, 18629.
(16) Marterny, A.; Lienau, C.; Zewail, A. H. *J. Phys. Chem.* **1996**, *100*, 18650.
(17) Liu, Q.; Wan, C.; Zewail, A. H. *J. Phys. Chem.* **1996**, *100*, 18666.
(18) Scherer, N. F.; Ziegler, L. D.; Fleming, G. R. *J. Chem. Phys.* **1992**, *96*, 5544.
(19) Scherer, N. F.; Jonas, D. M.; Fleming, G. R. *J. Chem. Phys.* **1993**, *99*, 153.
(20) Zadoyan, R.; Sterling, M.; Apkarian, V. A. *J. Chem. Soc., Faraday Trans.* **1996**, *92*, 1821.
(21) Smith, D. E.; Harris, C. B. *J. Chem. Phys.* **1987**, *87*, 2709.
(22) Harris, A. L.; Brown, J. K.; Harris, C. B. *Annu. Rev. Phys. Chem.* **1988**, *39*, 341.
(23) Kelley, D. F.; Abul-Haj, N. A.; Jang, D. J. *J. Chem. Phys.* **1984**, *80*, 4105.
(24) Abul-Haj, N. A.; Kelly, D. F. *J. Chem. Phys.* **1986**, *84*, 1335.
(25) Harris, A. L.; Berg, M.; Harris, C. B. *J. Chem. Phys.* **1986**, *84*, 788.
(26) Hippler, H.; Luther, K.; Troe, J. *Ber. Bunsen-Ges. Phys. Chem.* **1973**, *77*, 1104.
(27) Luther, K.; Troe, J. *Chem. Phys. Lett.* **1974**, *24*, 85.
(28) Troe, J. *Annu. Rev. Phys. Chem.* **1978**, *29*, 223.
(29) Luther, K.; Schroeder, J.; Troe, J.; Unterberg, U. *J. Phys. Chem.* **1980**, *84*, 3072.
(30) Otto, B.; Schroeder, J.; Troe, J. *J. Chem. Phys.* **1984**, *81*, 202.
(31) Hippler, H.; Schubert, V.; Troe, J. *J. Chem. Phys.* **1984**, *81*, 3931.
(32) Hippler, H.; Otto, B.; Schroeder, J.; Schubert, V.; Troe, J. *Ber. Bunsen-Ges. Phys. Chem.* **1985**, *89*, 240.
(33) Troe, J. *J. Phys. Chem.* **1986**, *90*, 357.
(34) Dupuy, C.; van den Bergh, H. *Chem. Phys. Lett.* **1978**, *57*, 348.
(35) Zellweger, J. M.; van den Bergh, H. *J. Chem. Phys.* **1980**, *72*, 5405.
(36) Dutoit, J.-C.; Zellweger, J. M.; van den Bergh, H. *J. Chem. Phys.* **1983**, *78*, 1825.
(37) Bunker, D. L.; Jacobson, B. J. *J. Am. Chem. Soc.* **1972**, *94*, 1843.
(38) Murrell, J. N.; Stace, A. J.; Dannel, R. *J. Chem. Soc., Faraday Trans. 2* **1978**, 1534.
(39) Stace, A. J. *J. Chem. Soc., Faraday Trans. 2* **1981**, *77*, 2105.

(40) Lipkus, A. H.; Buff, F. P.; Sceats, M. G. *J. Chem. Phys*. **1983**, *79*, 4830.
(41) Ali, D. P.; Miller, W. H. *J. Chem. Phys*. **1983**, *78*, 6640.
(42) Brooks, C. L.; Balk, M. W.; Adelman, S. A. *J. Chem. Phys*. **1983**, *79*, 784.
(43) Valentini, J. J.; Cross, J. B. *J. Chem. Phys*. **1982**, *77*, 572.
(44) Beswick, J. A.; Monot, R.; Philippoz, J.-M.; van den Bergh, H. *J. Chem. Phys*. **1987**, *86*, 3965.
(45) Valentini, J. J.; Cross, J. B. J. *Chem. Phys*. **1982**, *77*, 572.
(46) Skene, J. M.; Lester, M. I. *Chem. Phys. Lett*. **1985**, *116*, 93.
(47) Saenger, K. L.; McCleland, G. M.; Herschbach, D. R. *J. Phys. Chem*. **1981**, *85*, 3333.
(48) Burke, M. L.; Klemperer, W. *J. Chem. Phys*. **1993**, *98*, 6642.
(49) NoorBatcha, I.; Raff, L. M.; Thompson, D. L. *J. Chem. Phys*. **1984**, *81*, 5658.
(50) Garca-Vela, A.; Villarreal, P.; Delgado-Barrio, G. *J. Chem. Phys*. **1991**, *94*, 7868.
(51) Li, Z.; Borrmann, A.; Martens, C. C. *J. Chem. Phys*. **1992**, *97*, 7234.
(52) Dardi, P. S.; Dahler, J. S. *J. Chem. Phys*. **1990**, *93*, 242.
(53) Eichler, H. J.; Gunter, P.; Pohl, D. W. *Laser Induced Dynamic Gratings*; Springer-Verlag: Berlin, 1986.
(54) Zhu, X. R.; Harris, J. M. *Chem. Phys*. **1991**, *157*, 409.
(55) Zhu, X. R.; Harris, J. M. *Chem. Phys. Lett*. **1991**, *186*, 183.
(56) Kimura, Y.; Sugihara, K.; Terazima, M.; Hirota, N. *Bull. Chem. Soc. Jpn*. **1997**, *10*, 2627.
(57) Paige, M. E.; Harris, C. B. *Chem. Phys*. **1990**, *149*, 37.
(58) Sceats, M. G.; Dawes, J. M.; Millar, D. P. *Chem. Phys. Lett*. **1985**, *114*, 63.
(59) Yoshimura, Y.; Nakahara, M. *J. Chem. Phys*. **1984**, *81*, 5679.
(60) Terazima, M.; Azumi, T. *Bull. Chem. Soc. Jpn*. **1989**, *62*, 2862.
(61) Yamaguchi, S.; Hirota, N.; Terazima, M. *Chem. Phys. Lett*. **1998**, *286*, 284.
(62) Kimura, Y.; Kanda, D.; Terazima, M.; Hirota, N. *Ber. Bunsen-Ges. Phys. Chem*. **1995**, *99*, 196.
(63) Yamaguchi, T.; Kimura, Y.; Hirota, N. *J. Phys. Chem. A* **1997**, *101*, 9053.
(64) (a) Ar. Twu, C. H.; Lee, L. L.; Starling, K. E. *Fluid Phase Equilib*.**1980**, *4*, 35. (b)Xe and Kr. Rabinovich, V. A.; Vasserman, A. A.; Nedstup, V. I.; Veksler, L. S. *Thermophysical Properties of Neon, Argon, Krypton, and Xenon*; Hemisphere Publishing Corporation: Washington, DC, 1988. (c) CO_2. Huang, F. H.; Li, M. H.; Starling, K. E.; Chun, F. T. H. *J. Chem. Eng. Jpn*. **1985**, *18*, 490. (d) C_2H_6. Younglove, B. A.; Ely, J. F. *J. Phys. Chem. Ref. Data* **1987**, *16*, 577. (e) N_2O. Yokoyama, C.; Takahashi, M.; Takahash, S. *Int. J. Thermophys*. **1994**, *15*, 603. (f) SF_6. Morsy, T. E. *J. Chem. Eng. Data* **1970**, *15*, 256. (g) C_7H_{16}. Otto, B.; Schroeder, J.; Troe, J. *J. Chem. Phys*. **1984**, *81*, 202.
(65) We could not determine the concentration of I_2 in the case of fluids at high pressures owing to the adsorption of I_2 at the O-ring of the pressure seal. The optical density of the solution was around 1−1.5 with a 1 cm path length at the peak maximum.
(66) Kimura, Y.; Yamaguchi, T.; Hirota, N. Manuscript in preparation.
(67) Demtröder, W. *Laser Spectroscopy*, 3rd ed.; Springer-Verlag: Berlin, 1988. Kronig, R. L. *J. Opt. Soc. Am*. **1926**, *12*, 547. Kramers, H. A. *Atti Congr. Int. Fis*. **1927**, *2*, 545.
(68) We have used the values of $\rho = 0.6594$ g/cm^3, $C_p = 143.2$ J K^{-1} mol^{-1}, $dn/dT = -5.2 \times 10^{-4}$ K^{-1}. These values are taken from ref 69.
(69) Riddck, J. A.; Bunger, W. B. *Techniques of Chemistry*, 3rd ed.; Wiley: New York, 1970; Vol. 2. *Landolt-Börnstein, II Band*; Springer-Verlag: Berlin, 1962.
(70) Each transient was fit with eq 12 in the time range until the intensity becomes the half of its initial value. In several cases, we omit the initial part of the transient to eliminate the effect of the scattering of the pump beam.
(71) Yoshimura, Y.; Kimura, Y.; Nakahara, M. *Ber. Bunsen-Ges. Phys. Chem*. **1988**, *92*, 1095.
(72) Weast, R. C. *Handbook of Chemistry and Physics*; CRC Press: Boca Raton, FL, 1989.
(73) Fernandez, D. P.; Fernandez-Perini, R. *J. Chem. Thermodyn*. **1992**, *24*, 377.
(74) Besserer, G. J.; Robinson, D. B. *J. Chem. Eng. Data* **1973**, *18*, 137.
(75) The Japan Society of Mechanical Engineers. *JSME Data Book: Thermophysical Properties of Fluids*; Maruzen: Japan, 1983.
(76) Kimura, Y.; Yoshimura, Y.; Nakahara, M. *J. Chem. Phys*. **1989**, *990*, 5679.
(77) Kimura, Y.; Yoshimura, Y. *J. Chem. Phys*. **1992**, *96*, 3085.
(78) Kimura, Y.; Yoshimura, Y. *J. Chem. Phys*. **1992**, *96*, 3824.
(79) Hippler, H.; Schubert, V.; Troe, J. *Ber. Bunsen-Ges. Phys. Chem*. **1985**, *89*, 760.
(80) Schwarzer, D.; Troe, J.; Votsmeier, M.; Zerezke, M. *J. Chem. Phys*. **1996**, *105*, 3121.
(81) Schwarzer, D.; Troe, J.; Zerezke, M. *J. Chem. Phys*. **1997**, *107*, 8380.
(82) Yamaguchi, T.; Kimura, Y.; Hirota, N. *Mol. Phys*. **1998**, *3*, 527.
(83) Roessling, G. L.; Franck, E. U. *Ber. Bunsen-Ges. Phys. Chem*. **1983**, *77*, 882.
(84) Hirschfelder, J. O.; Curtis, C. F.; Bird, R. B. In *Molecular Theory of Gases and Liquids*; Wiley: New York, 1954.
(85) Braune, H.; Strassmann, F. *Z. Phys. Chem*. **1928**, *143A*, 225.
(86) Fernandez, D. P.; Fernandez-Prini, R. *Ber. Bunsen-Ges. Phys. Chem*. **1993**, *97*, 1000.
(87) Both in CO_2 and in Xe, the solibility shows a good linear dependence on the solvent density. The data of Xe are taken from the polynomial expansion for the logarithm of the solubility in the density over 2.5 mol/L. The extrapolation of their results gives a good limiting value at the vapor. We used the value of 51.5 cm^3 mol^{-1} for V_s.
(88) From viscosity data. Reid, R. C.; Praunitz, J. M.; Poling, B. E. *The Properties of Gases & Liquids*; McGraw-Hill: New York, 1988.
(89) Papanikolas, J. M.; Gord, J. R.; Levinger, N. E.; Ray, D.; Vorsa, V.; Lineberger, W. C. *J. Phys. Chem*. **1991**, *95*, 8028.
(90) Kofke, D. A. *J. Chem. Phys*. **1993**, *98*, 4149.
(91) Kimura, Y.; Yoshimura, Y. *Mol. Phys*. **1991**, *72*, 297.